EPR Centers for Nickel Substitutional impurity in diamond

A. M. Gsiea, M. K. Atumi

Physics Department, Faculty of Education Tripoli, University of Tripoli, Tripoli, Libya.

Email: a.gsiea@uot.edu.ly

Abstract:

We present a first-principles density functional theory study of nickel impurities in diamond. The atomic structures, formation and transition energies, and hyperfine parameters of nickel substitutional were computed using ab initio total energy methods. Based upon Local density functional theory, our calculations were in excellent agreement with one interpretation of electron paramagnetic resonance of nickel in diamond.

1. Introduction:

By using high pressure, high temperature, and transition metal alloys (TM) containing manganese, iron, nickel, and cobalt as catalysts, high quality synthetic diamond can be created from graphite [1]. However, transition metals may be added to the resultant crystal [2–5], often produce active centers with observable spectral absorption bands. The only TM that has been clearly detected as being present in the final synthetic material is nickel. Measurements of optical absorption and electron paramagnetic resonance, or EPR, have revealed active centers connected to isolated Ni [4, 5] and Ni-related complexes with intrinsic defects or dopants [6]. The microscopic make-up of those centers, however, is a subject of great debate.

By using EPR [4] and optical measurements [7], isolated nickel in diamond has been shown to have a tetrahedral symmetry and a spin (3/2). The solitary substitutional nickel in the negative charge state (Ni_s^{-1}) with a $3d^7$ configuration has been theorized to create this center, designated W8 [4]. The NIRIM-1 and NIRIM-2 centers were discovered by EPR examinations to be two more significant active diamond centers [5]. At low temperatures (T=25 K), the NIRIM-1 core has been identified as having a spin (1/2) in a trigonal symmetry, and at higher temperatures, in a tetrahedral symmetry. According to one interpretation, this center is the consequence of a single nickel interstitial particle in the positive charge state (Ni_i^+) with a $3d^9$ configuration. With a spin 1/2 and trigonal symmetry, the NIRIM-2 center has been found by EPR [5] and optical [8, 9] observations. For this center's a number of microscopic models have been suggested. It has

been hypothesized that the configuration might involve an interstitial nickel in a strong trigonal field, induced by a neighboring vacancy or impurity, taking into consideration the g values (g=2.32 and g =0) found for this center [5].

2. Method:

Calculations are based upon density functional theory using the AIMPRO package [10, 11]. Defects are simulated by the use of large super-cells and periodic boundary conditions. The cells are repeats of the primitive fcc unit cell containing eight atoms of carbon. The calculated values for constant lattice is 3.53 Å. We have analysed Ni-centers in super-cells containing 64 atoms, comprised from (2 × 2 × 2) primitive cells. Table (1) presents the theoretical results of crystalline diamond compared to the experimental data [12].

The Brillouin-zone is sampled using the Monkhorst-Pack [13] scheme generally with a mesh of 2×2×2 k-points. Structures are optimized via a conjugate-gradients scheme until the change in energy between iterations is less than 10^{-5} Ha.

Atoms are simulated using ab initio pseudo-potentials [14] and the total energies and forces are obtained with a local density approximation for the exchange-correlation [15]. The wave functions and charge density are expanded in terms of Gaussian orbitals and plane-waves, respectively [16].

For the C and Ni we include s, p and d functions, with a total of 28 and 32 functions per atom, respectively. Plane waves up to 150 Ha are used to expand the charge density. We calculate the formation energy of a defect X using

$$E^f(X, q) = E^{tot}(X, q) - \sum \mu_i + q(E_v(X, q) + \mu_e) + \zeta(X, q) \quad (1)$$

Where $E^{tot}(X, q)$ is the total energy calculated of the system X containing the defect in charge state q, μ_i denotes the chemical potential of species (i = C and Ni) , $E_v(X, q)$ is the Fermi energy at the valance-band top, μ_e is the electron chemical potential, which defined as zero at the valence band top. The chemical potential for Ni is taken Ni metal.

For the electrical characteristics of the defect centers, we calculate the transition levels, E(q;q') defined as the electron chemical potential where the formation energies for

two charge states, q and q', are equal. For example, the donor level is the value of μ_e for which $E^f(X;0)=E^f(X;+1)$, and $E^f(X;0)=E^f(X;-1)$ for acceptor level.

Tab. 1: Theoretical structural and electronic properties of diamond: lattice constant (a), bulk modulus (B), and energy band gap (E_g).

	A (Å)	B (Mbar)	E_g (eV)
This work	3.53	4.48	4.5
Expt.[12]	3.567	4.42	5.48

3. Result and Discussion:

Substitutional Nickels (Ni_s)

Relaxation of Nickel impurity substitute diamond has been examined. In the final relaxed configuration, the structure obtained for neutral Ni_s^0 is shown in (Fig 1). The nickel atom remains on-site and is a tetrahedral symmetry with four neighbor carbon atoms, the distance between Ni_s^0 and the first neighbor is 1.75 Å moving outward on its by 0.22 Å , in excellent agreement with previous calculation [17–19, 22].

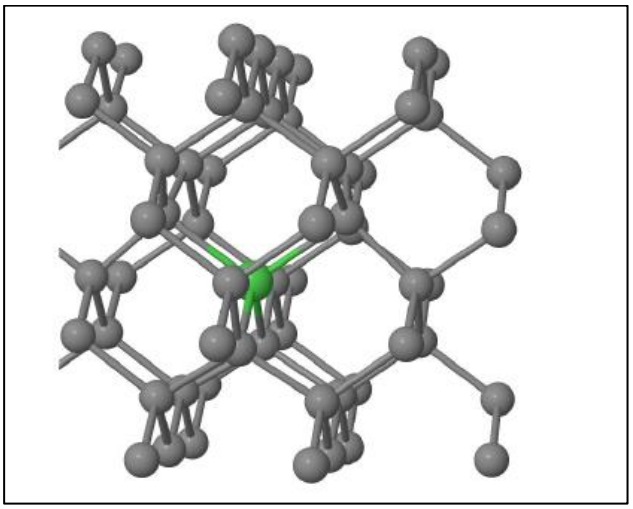

Fig. 1: Schematic structures of (Ni_C)

However, for neutral charge state the different energies between spin S=1 and spin S=0 is small at 0.13 eV where they have T_d symmetry. Further-more the different energies between Td symmetry and C_{3v} for Ni_s^{+1} are small at 0.01 eV.

By calculating the formation energy as a function of charge state and μ_e, we can estimate the electrical levels of Ni_S. The charge-dependent formation energies yield both donor and acceptor levels in the band-gap which are summarized in (Fig 2).

The donor levels are calculated at around E_v+1.6 eV and E_v+0.7 eV for (0/+) and (+1/+2) transitions, respectively. The acceptor transition energy (0/-) of the Ni_s is E_v+3.0 eV where E_v defines the valance band top.

This value is in excellent agreement with the experimental value of E_v+3.0 eV [20, 21], and theoretical value of E_v+2.9 eV [17, 18].

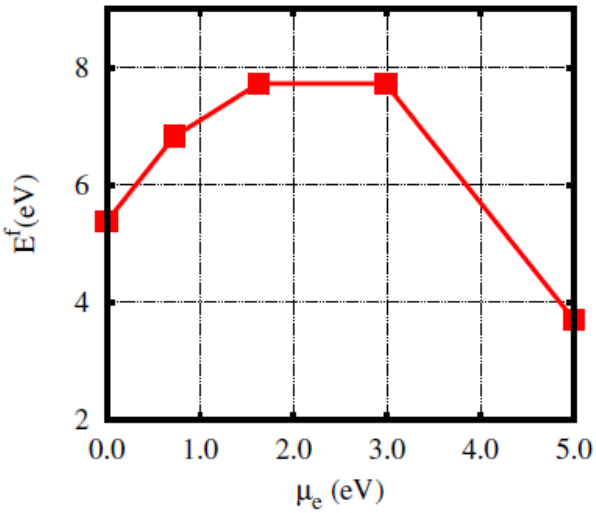

Fig. 2: Plot of E^f vs. μ_e for (Ni) defects in diamond calculated using the 64 atom super-cell with different charge state.

The negative substitutional nickel center (Ni_s^{-1}) has a T_d symmetry as well and presents an affective spin S=3/2, while in the positive charge state (Ni_s^{+1}) it has C_{3v} symmetry and presents an effective spin S=1/2. The electric level properties of nickel impurity substitutional diamond are further illustrated in (Fig 3), which shows the band-structure along high-symmetry directions in the Brillouin-Zone.

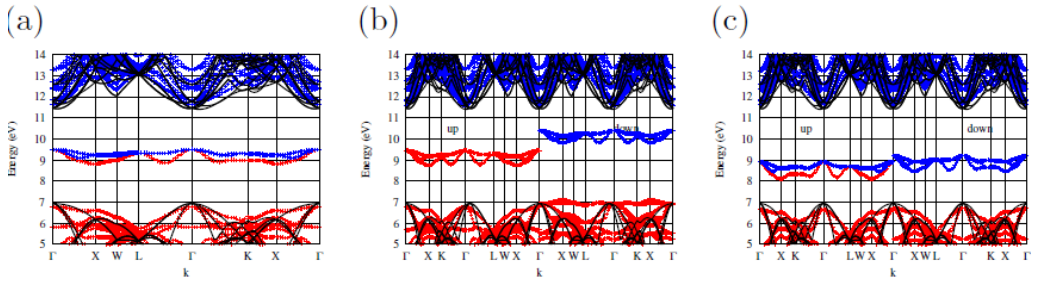

Fig. 3: Plot of the band structure of Ni_s in (a) the Neutral charge state (b) the positive charge state (c) the negative charge state. where the zero of energy is set to be the valance band top for bulk diamond. Red and blue crosses indicate filled and empty bands, respectively, while black lines indicates the comparable bands of defect free diamond.

Combining the formation energy and band structure data strongly suggests that nickel substitutional diamond is thermodynamically stable at neutral, positive and negative charge state. Table 2 shows the symmetry, spin, and transition energies for all the centers nickel substitutional diamond.

Tab. 2: Results for substitutional Ni in different charge states. The table presents the symmetry, spin (S), and transition energies (E_t with relation to E_v)

	Symmetry.	Spin	E_t (eV)
Ni_s^0	T_d	0	
Ni_s^{+1}	C_{3v}	1/2	1.6 (0/+)
Ni_s^{+2}	C_{3v}	0	0.7(+1/+2)
Ni_s^{-1}	T_d	3/2	3.0(-/0)

The hyperfine interactions between the unpaired electron and nuclear of the C^{13} in the defect are modeled [23]. Table (3) presents the hyperfine parameters in the nickel impurity and in its neighbors for all the centers studied here.

Tab. 3: Calculated hyperfine parameters (A), given in MHz, in the N_i^{61} nucleus, in the NN and in the NNN C^{13} nuclei for the Ni_s^{+1} and Nis^{-1} centers. The table also presents the experimental A values for the W8 center. For the centers there are nonequivalent NNs and NNNs, which lead to different A values.

	Ni		NN		NNN		
	A_{II}	$A_{\perp}$	A_{II}	$A_{\perp}$	A_1	A_2	A_3
Ni_s^{+1}	23.34	23.34	45.67	14.46	13.22	13.34	15.42
Ni_s^{-1}	-18.42	-18.42	38.88	8.79	10.48	7.66	7.65
W8(Ni_s^{-1})	18.2	18.2	37.5	9.5	10.7	7.6	7.5

4. Summary:

We investigated the electrical and structural characteristics of isolated nickel impurities in diamond using total energy ab initio methods. The EPR results of the W8 center are completely compatible with our results for the nickel substitutional center. We suggest that a solitary substitutional nickel in the positive charge state might constitute the microscopic structure of the NIRIM-1 core. The NIRIM-2 center's EPR results also reveal a potent trigonal field. A neighboring vacancy or impurity and an interstitial nickel atom were previously proposed as the components of this center. We demonstrated that the microscopic structure of the NIRIM-2 center could not be a complex made up of an interstitial nickel and a vacancy because it is unstable and turns into a nickel substitute. However, without any crystallographic deformation caused by a vacancy or impurity, isolated interstitial nickel in the positive charge state alone was unable to explain the experimental results for the NIRIM-2 center.

References:

[1] J. C. Angus, and C. C. Hayman, Science. 214, 913 (1988).

[2] G. Davies, A. J. Neves, and M. H. Nazare, Europhys Lett. 9, 47 (1989).

[3] D. J. Twitchen, J. M. Baker, M. E. Newton, and K. Johnston, Phys. Rev. B 61, 9 (2000).

[4] J. Isoya, H. Kanda, J. R. Norris, J. Tang, and M. K. Bowman, Phys. Rev. B 41, 3905 (1990).

[5] J. Isoya, H. Kanda, and Y. Uchida, Phys. Rev. B 42, 9843 (1990).

[6] V. A. Nadolinny, A. P. Yelisseyev, J. M. Baker, M. E. Newton, D. J. Twitchen, S. C. Lawson, O. P. yuryeva, and B. N. Feigelson, J. Phys. Condens. Matter 11, 7357 (1999).

[7] M. H. Nazare, J. C. Lopes, and A. J. Neves, Physica B 308-310, 616 (2001).

[8] M. H. Nazare, A. J. Neves, and G. Davies Phys. Rev. B 43, 14196 (1991).

[9] P. W. Mason, F. S. Ham, and G. D. Watkins, Phys. Rev. B 49, 5417 (1999).

[10] P. R. Briddon and R. Jones, Phys. Status Solidi B 217, 131 (2000).

[11] M. J. Rayson and P. R. Briddon, Computer Phys. Comm. 178, 128 (2008).

[12] Landolt-BÖrnstein, Numerial Data and Functional Relation- ships in Science and Technology, vol. 17, edited by O. Madelung, M. Schulz, and H. Weiss (Springer-Verlag, New York, 1982).

[13] H. J. Monkhorst and J. D. Pack, Phys. Rev. B 13, 5188 (1976).

[14] N. Troullier and J. L. Martins, Phys. Rev. B 43, 1993 (1991).

[15] J. P. Perdew and Y. Wang, Phys. Rev. B 45, 13244 (1992).

[16] J. P. Goss, M. J. Shaw, and P. R. Briddon, Topics in Appl. Phys. 104,69 (2007).

[17] J. P. Goss, P. R. Briddon, R. Jones and S. Oberg J. Phys. Condens. Matter 16, 4567-4578 (2004).

[18] R. Larico, J. F. Justo, W. V. M. Machado, and L. V. C. Assali, Brazilian Journal of Physics 34, 669 (2004).

[19] Kenji. Tsuruta, Satoshi. Emoto, Chieko. Totsuji, and Hiroo. Totsuji, Computational Material Science 38, 873-882 (2007).

[20] D. M. Hofmann, P. Christmann, D. Volm, K. Pressl, L. Pereira, L. Santos, and E.Pereira, Mater Sci. Forum 196-201, 79 (1995).

[21] D. M. Hofmann, M. Ludwing, P. Christmann, D. Volm, B. K. Meyer, L. Pereira, L. Santos, and E.Pereira, Phys. Rev. B 50, 17618 (1994).

[22] R. Larico, L. V. C. Assali, W. V. M. Machado, and J. F. Justo, Compu. Mater. Sci. 30, 62-66 (2004).

[23] M.K. Atumi, J.P. Goss, P.R. Briddon, A.M. Gsiea, and M.J. Rayson, Result in Physics 16, 102860 (2020).